

# A DFT Study of the Structures of N<sub>2</sub>O Adsorbed on the Pd(110) Surface

Anton Kokalj\* and Ivan Kobal

Jožef Stefan Institute, 1000 Ljubljana, Slovenia

Tatsuo Matsushima

Catalysis Research Center, Hokkaido University, Sapporo 060-0811, Japan

Received: August 2, 2002; In Final Form: October 29, 2002

The adsorption of nitrous oxide N<sub>2</sub>O on the Pd(110) surface has been studied and characterized using density-functional theory. We found that N<sub>2</sub>O binds weakly to the surface in two alternative forms, either tilted with the terminal N atom attached to the surface or lying horizontally on the surface in the [001] direction. The adsorption on the on-top site is more stable than that on the bridge one. The horizontal form of N<sub>2</sub>O(a) is appropriate as the precursor of the inclined desorption of the product N<sub>2</sub> observed in the thermal decomposition of N<sub>2</sub>O(a).

## 1. Introduction

Nitrous oxide, N<sub>2</sub>O, has attracted increasing attention as a greenhouse gas and also as an intermediate in the removal of NO<sub>x</sub> on automobile three-way catalysts. However, the mechanism of its decomposition and formation on the catalysts is not yet clear. For this reason, and also because—to the best of our knowledge—our previous report<sup>1</sup> is the only one to contain theoretical calculations of the interaction of N<sub>2</sub>O with the transition metal surfaces, we have performed calculations on the basis of density functional theory (DFT) in order to characterize in detail the adsorption structures of N<sub>2</sub>O(a) on the fcc (110) transition metal surface.

Recently, nitrogen molecules produced on some fcc (110) surfaces were observed to desorb in inclined bidirectional lobes in a plane in the [001] and [00 $\bar{1}$ ] directions. The processes investigated so far are the thermal dissociation of N<sub>2</sub>O on Pd,<sup>2–7</sup> Rh,<sup>8</sup> and Ir,<sup>8</sup> the thermal decomposition of NO on Pd,<sup>2,6,9,10</sup> and the steady-state NO + CO reaction on Pd.<sup>6,11–13</sup> By using isotope tracers, Ikai and Tanaka clearly showed that, on Pd(110), desorbing N<sub>2</sub> molecules, from the recombination reaction of 2N(a)  $\rightarrow$  N<sub>2</sub>(g) collimated sharply along the surface normal, whereas N<sub>2</sub> from NO decomposition desorbed in an inclined direction.<sup>14</sup> Haq and Hodgson suggested that the inclined desorption of N<sub>2</sub> was due to locally reconstructed or corrugated patches induced by N<sub>2</sub>O adsorption.<sup>15</sup> However, in both the steady-state NO + CO reaction and N<sub>2</sub>O decomposition at around 100 K on Pd(110), no relation was found between surface reconstruction and the inclined desorption.<sup>5,13</sup> This indicates that the inclined desorption of N<sub>2</sub>, induced in N<sub>2</sub>O(a) dissociation events, takes place on the nonreconstructed surface. By analogy to the photon-induced inclined desorption,<sup>16</sup> N<sub>2</sub>O oriented along the [001] direction was proposed to be the state immediately preceding N<sub>2</sub> emission.<sup>2</sup> The possibility of N<sub>2</sub>O being adsorbed in a tilted form with its O atom attached to the surface was not rejected since it easily explained the inclined desorption.<sup>17</sup>

The structure of N<sub>2</sub>O(a) immediately before dissociation can be studied only by means of theoretical calculations. In our previous contribution<sup>1</sup> we reported some results for N<sub>2</sub>O on Pd(110), predicted by the DFT. These calculations were limited to a high coverage, while in this study the calculations are performed over a wider range of coverage, and the stability of adsorbate on different sites and adsorbate orientations are thoroughly examined. In particular, inclined desorption was only observed at lower adsorbate coverage, indicating that it is dependent on the coverage. For this reason, an analysis of structural and energetic differences of adsorption at different coverages has been carried out.

## 2. Technical Details

Our calculations were performed in the framework of DFT, using the generalized gradient approximation (GGA) of Perdew–Burke–Ernzerhof (PBE).<sup>18</sup> Nuclei and core electrons were described by ultrasoft pseudopotentials.<sup>19</sup> The Kohn–Sham orbitals were expanded in a plane-wave basis set with a kinetic energy cutoff of 27.5 Ry (220 Ry for the charge-density cutoff). Brillouin-zone (BZ) integrations have been performed with the special-point technique,<sup>20</sup> whereas the Fermi surface has been treated with a smearing parameter<sup>21</sup> of 0.03 Ry. All calculations in this work have been done using the PWSCF package,<sup>22</sup> while figures of the chemical structures and electronic charge densities were produced by the XCRYSDEN<sup>23–26</sup> graphical package.

The perfect Pd(110) surface was modeled with a slab consisting of five palladium (110) layers, and the N<sub>2</sub>O molecule was adsorbed on one side of the slab. The adsorption phenomena were modeled by super-cells of different surface geometries (see Figure 1). In particular, N<sub>2</sub>O adsorption was modeled at 0.5 and 0.25 monolayer (ML) coverages. Adsorption at 0.5 ML coverage was modeled by (2  $\times$  1) and c(2  $\times$  2) super-cells, and the BZ integrations were performed with a 4  $\times$  6 and 5  $\times$  5 Monkhorst–Pack mesh, respectively. The 0.25 ML adsorption was modeled by (2  $\times$  2) and c(2  $\times$  4) super-cells, where 4  $\times$  3 and 3  $\times$  3 Monkhorst–Pack meshes were used respectively for BZ integrations. In matrix notation the c(2  $\times$  2) and c(2  $\times$  4) super-cells can be written as  $\begin{pmatrix} 1 & 1 \\ -1 & 1 \end{pmatrix}$  and  $\begin{pmatrix} 1 & 2 \\ -1 & 2 \end{pmatrix}$ , respectively. The thickness of the vacuum (the distance between N<sub>2</sub>O

\* Corresponding author. Address: Jožef Stefan Institute, POB 3000, SI-1001 Ljubljana, Slovenia. Tel: +386-1-477-35-23. Fax: +386-1-477-38-11. E-mail: Tone.Kokalj@ijs.si. WWW: <http://www-k3.ijs.si/kokalj/>.

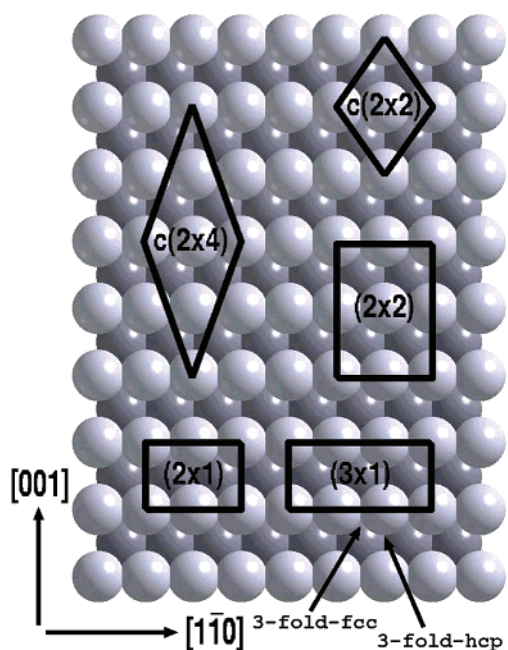


**Figure 1.** A model of the Pd(110) surface with the definition of the [001] and [110] crystal axes. Surface super-cells used in this work are also shown.

molecule and the adjacent slab) was set to about 8 Å. We used the calculated bulk lattice parameter as the in-plane lattice spacing. The structure of the bottom three layers of the slab was fixed with the bulk inter-plane spacing, whereas the geometry of the top two layers and N<sub>2</sub>O molecule was optimized.

The binding energy ( $E_b$ ) of adsorbed N<sub>2</sub>O was calculated as  $E_b = (E_{\text{sub}} + E_{\text{N}_2\text{O}}) - E_{\text{N}_2\text{O}/\text{sub}}$ , where  $E_{\text{sub}}$ ,  $E_{\text{N}_2\text{O}}$ , and  $E_{\text{N}_2\text{O}/\text{sub}}$  are the total energies of the bare substrate, the isolated N<sub>2</sub>O molecule and the N<sub>2</sub>O/substrate adsorption system, respectively. With this definition, positive binding energies indicate attraction. For nondissociative molecular adsorption the binding energy is related to the experimentally measured heat of adsorption ( $\Delta H_{\text{ads}}$ ).

### 3. Results

**3.1. Isolated Constituents: Bulk Pd, Pd(110) Surface, and the N<sub>2</sub>O Molecule in the Gas Phase.** The experimental lattice parameter of bulk palladium is 3.89 Å,<sup>27</sup> whereas our GGA calculations yield 3.97 Å—an overestimation of 2.1%.

This agrees with the results obtained by the full-potential linearized augmented-plane-wave method (3.97 Å),<sup>28</sup> and by the linear-combination-of-atomic-orbitals method (3.95 Å).<sup>28</sup>

The properties of the clean Pd(110) surface have been calculated using 5-, 6-, and 7-layer slabs with a  $p(1 \times 1)$  surface geometry. All layers have been relaxed symmetrically here in order to obtain a meaningful estimation of the surface energy, and work functions. The surface energy  $E_{\text{surf}}$  was estimated using the relation  $E_{\text{surf}} = 1/2\{E_{\text{slab}}(N) - N[E_{\text{slab}}(N+1) - E_{\text{slab}}(N)]\}$ , where  $N$  is the number of layers. The work function  $\phi$  was calculated as the difference between the average electrostatic potential in the vacuum and the Fermi level. Our GGA calculations yielded  $E_{\text{surf}} = 1.09$  eV/atom = 0.10 eV/Å<sup>2</sup> and  $\phi = 4.88$  eV. The calculated surface energy is in excellent agreement with the GGA value reported by Dong et al.,<sup>29</sup> while the calculated work function is lower than the experimental value of 5.25 eV.<sup>30</sup> The relaxations of the first ( $\Delta d_{12}$ ) and second ( $\Delta d_{23}$ ) layers were calculated to be -8.1% and +3.4%, respectively, while experimental values are  $\Delta d_{12} = -5.8\%$  and  $\Delta d_{23} = +0.7\%$ .<sup>31</sup>

For the N<sub>2</sub>O molecule in the gas-phase our calculations predict a linear geometry with a nitrogen–nitrogen distance ( $d_{\text{NN}}$ ) of 1.142 Å, and a nitrogen–oxygen distance ( $d_{\text{NO}}$ ) of 1.210 Å, which agree well with the B3LYP and MP2 calculated distances.<sup>32</sup> The experimental values are 1.128 Å for  $d_{\text{NN}}$  and 1.184 Å for the  $d_{\text{NO}}$  distance.<sup>27</sup>

**3.2. Adsorption Structures of N<sub>2</sub>O(a).** Several possible configurations of molecular adsorption on the Pd(110) surface were examined in order to determine the orientation and site preference of the N<sub>2</sub>O molecule. The adsorption of N<sub>2</sub>O was modeled by attaching the molecule to the surface by its terminal nitrogen atom as well as by its oxygen atom. We have also modeled adsorption with the N<sub>2</sub>O molecule lying horizontally on the surface.

Our calculations yield the attractive adsorbate–substrate interaction only when the molecule is adsorbed on the on-top or bridge sites (i) by the terminal nitrogen atom, or (ii) lying horizontally on the surface. In the former case, the molecule is adsorbed in a tilted fashion and its geometry remains linear. The  $d_{\text{NN}}$  and  $d_{\text{NO}}$  distances are almost unchanged on adsorption. Precise estimation of the tilt angle is difficult due to the flatness of the potential energy surface. In the second case, the geometry of the horizontally adsorbed N<sub>2</sub>O molecule is not linear but bent, with the O atom pointing toward the surface. Also the  $d_{\text{NN}}$  and  $d_{\text{NO}}$  distances are greater in the horizontal structures—an indication of larger charge back-donation into the antibonding  $3\pi$  molecular orbital.

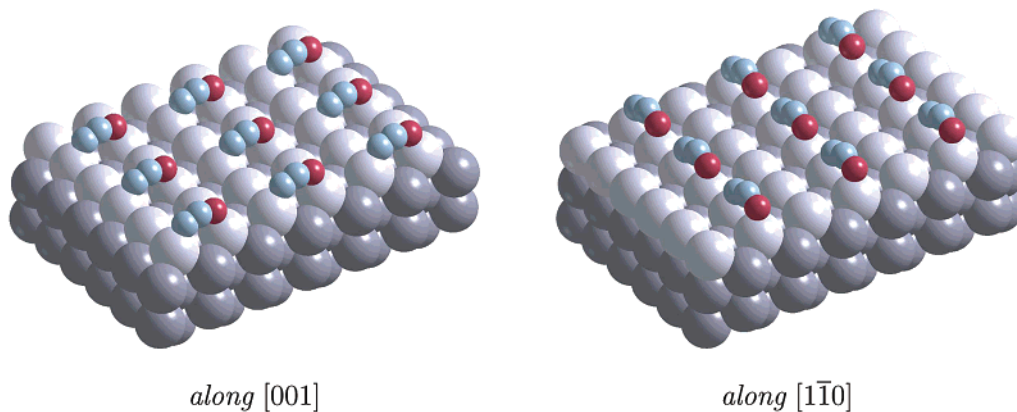


**Figure 2.** Ball model of optimized (2 × 2) horizontal N<sub>2</sub>O(a) moiety oriented along the [001] and [110] directions. Larger balls are Pd atoms, smaller blue balls are N atoms, and smaller red balls are O atoms.

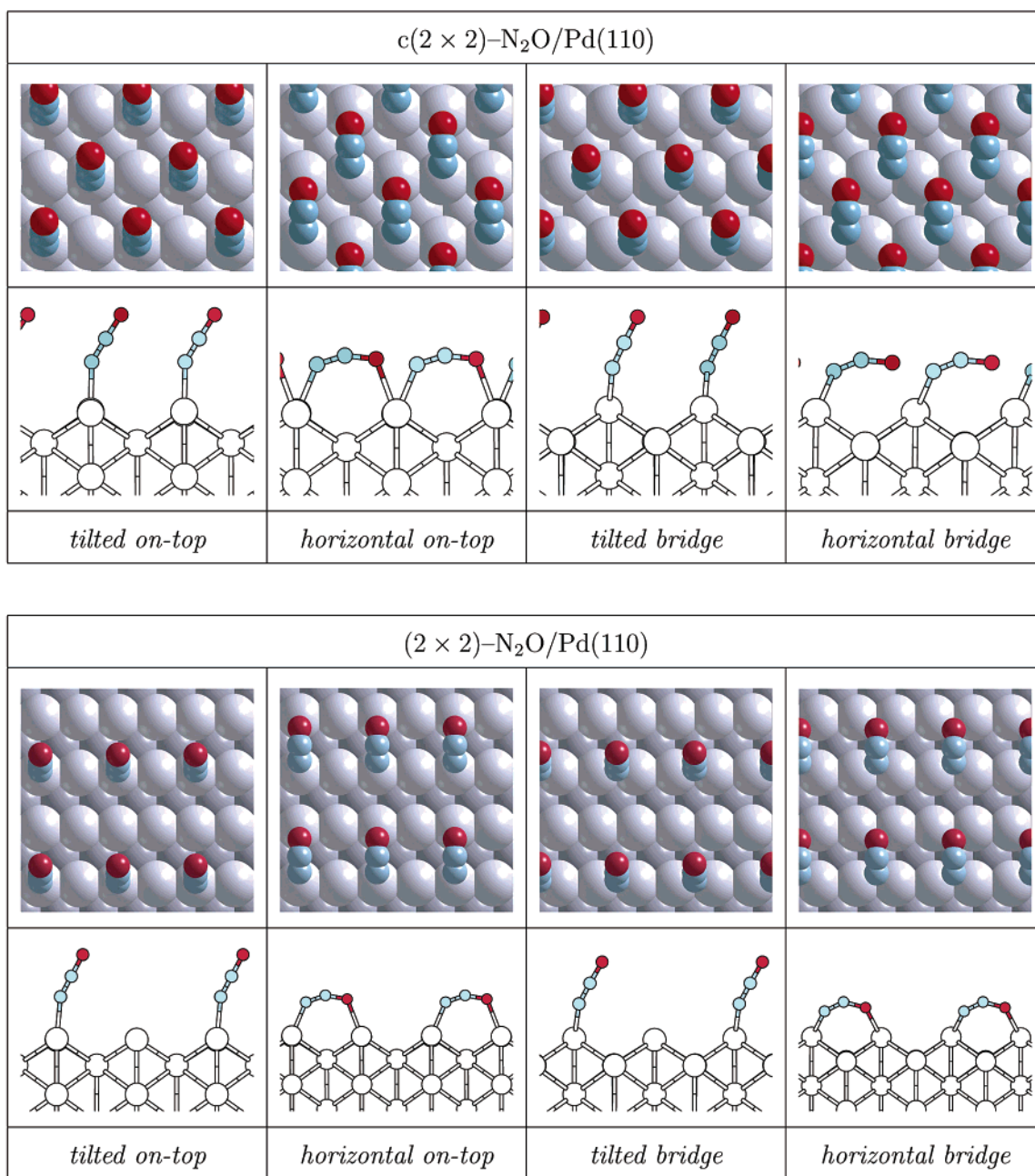


**Figure 3.** Top- and side-views of models of optimized N<sub>2</sub>O/Pd(110) structures for  $c(2 \times 2)$  and  $(2 \times 2)$  super-cells representing 0.5 and 0.25 ML coverage. Larger balls are Pd atoms, smaller blue balls are N atoms, and smaller red balls are O atoms.

**TABLE 1: Calculated Binding Energies ( $E_b$ ) and Structural Parameters of the on-Top Tilted and Horizontal N<sub>2</sub>O(a) Moieties Oriented in the [001] and [110] Directions<sup>a</sup>**

super-cell	site	orientation	$E_b$ (eV)	$d_{\text{PdN}}$ (Å)	$d_{\text{NN}}$ (Å)	$d_{\text{NO}}$ (Å)	$d_{\text{PdO}}$ (Å)	$\angle_{\text{Pd}^*\text{NN}}$ (deg)	$\angle_{\text{NNO}}$ (deg)	$\angle_{\text{NO}^*\text{Pd}}$ (deg)
$(2 \times 2)$	tilted on-top	[001]	0.36	2.09	1.15	1.21		157	180	
		[110]	0.27	2.11	1.15	1.21		152	179	
	horizontal on-top	[001]	0.40	2.07	1.17	1.23	2.27	132	151	121
		[110]	0.11	2.08	1.18	1.28	2.22	121	142	111
$(3 \times 1)$	horizontal on-top	[110]	0.19	2.08	1.18	1.27	2.22	121	142	111

<sup>a</sup> The labels  $d_{\text{PdN}}$ ,  $d_{\text{NN}}$ ,  $d_{\text{NO}}$ , and  $d_{\text{PdO}}$  stand for the distances between the corresponding atoms. The labels  $\angle_{\text{Pd}^*\text{NN}}$ ,  $\angle_{\text{NNO}}$ , and  $\angle_{\text{NO}^*\text{Pd}}$  stand for the corresponding angles. The symbol Pd\* (or \*Pd) stands either for the Pd atom (i.e., for on-top structures) or for the midpoint between the two bridging Pd atoms (i.e., for bridge structures). Hence, the symbol  $\angle_{\text{Pd}^*\text{NN}}$  corresponds to the Pd–N–N angle for the on-top structures, while for the bridge structures it corresponds to the angle between the “bridge-midpoint”–N–N.

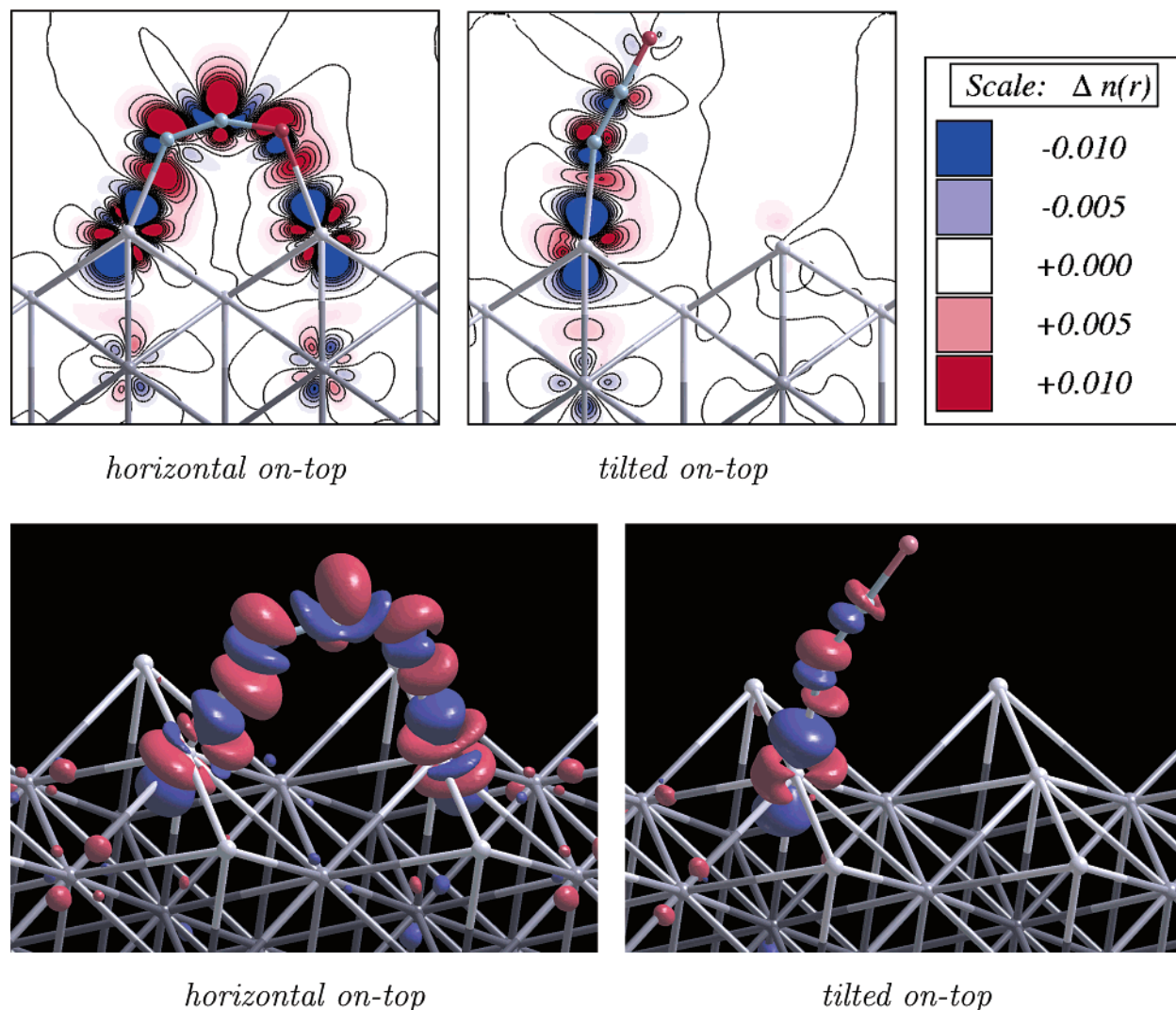
In the following text the term *horizontal on-top* will be used for horizontal N<sub>2</sub>O(a) which is adsorbed with its terminal N atom on top of a Pd atom and with its O atom on top of another Pd atom. In an analogous fashion, the term *horizontal*

*bridge* will be used for horizontally adsorbed N<sub>2</sub>O(a) with its terminal N atom on a short bridge site between two Pd atoms and its O atom on another short bridge site (see for example Figure 3).



**TABLE 2: Calculated Binding Energies ( $E_b$ ) and Structural Parameters of  $N_2O/Pd(110)$  Adsorption Systems for Several Surface Super-Cell Geometries Representing 0.5 and 0.25 ML coverage<sup>a</sup>**

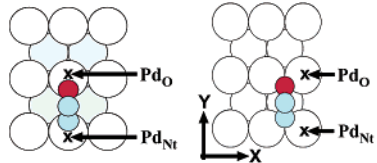
super-cell	site	$E_b$ (eV)	$d_{PdN}$ (Å)	$d_{NN}$ (Å)	$d_{NO}$ (Å)	$d_{PdO}$ (Å)	$\angle_{Pd^*NN}$ (deg)	$\angle_{NNO}$ (deg)	$\angle_{NO^*Pd}$ (deg)
$(2 \times 1)$	tilted on-top	0.38	2.11	1.15	1.21		152	179	
	tilted bridge	0.29	2.23	1.16	1.22		158	178	
$c(2 \times 2)$	tilted on-top	0.39	2.11	1.15	1.21		150	179	
	horizontal on-top	0.38	2.10	1.17	1.24	2.33	130	156	116
	tilted bridge	0.32	2.23	1.16	1.21		160	178	
	horizontal bridge	0.18	2.28	1.18	1.25	2.62	136	153	120
$(2 \times 2)$	tilted on-top	0.36	2.09	1.15	1.21		157	180	
	horizontal on-top	0.40	2.07	1.17	1.23	2.27	132	151	121
	tilted bridge	0.29	2.22	1.16	1.21		160	178	
	horizontal bridge	0.27	2.13	1.20	1.32	2.30	143	135	132
$c(2 \times 4)$	horizontal on-top	0.40	2.07	1.17	1.26	2.26	131	151	121
$N_2O(g)$				1.14	1.21			180	

<sup>a</sup> Labels have the same meaning as in Table 1.**Figure 4.** Charge density difference,  $\Delta n(\mathbf{r}) = n_{N_2O/sub}(\mathbf{r}) - [n_{sub}(\mathbf{r}) + n_{N_2O}(\mathbf{r})]$ , for the horizontal on-top (first row panels) and tilted on-top (second row panels)  $(2 \times 2)-N_2O/Pd(110)$  structures. The contours are drawn in linear scale from  $-0.01$  to  $0.01$   $e/a_0^3$ , with the increment of  $0.002$   $e/a_0^3$ , and isosurfaces of  $\pm 0.005$   $e/a_0^3$  are shown. The charge flows from blue to red regions.

The adsorption of horizontal on-top  $N_2O(a)$  was modeled oriented either along the  $[001]$  or along the  $[1\bar{1}0]$  directions (see Figure 2). Orientation along  $[001]$  was found to be more stable. The same orientation is also preferred for the tilted  $N_2O(a)$ . Table 1 displays the binding energies and the structural parameters of the two  $N_2O(a)$  forms adsorbed on the on-top

site at 0.25 ML coverage (i.e.,  $(2 \times 2)$  super-cell) and oriented in the  $[001]$  and  $[1\bar{1}0]$  directions.

Because the preferred orientation of  $N_2O(a)$  is in the  $[001]$  direction, the rest of the text will refer to this orientation. Table 2 summarizes the results of our adsorption calculations for various super-cells representing 0.5 and 0.25 ML coverage. The

**TABLE 3: Buckling of Surface Pd Atoms Induced by the Adsorption of N<sub>2</sub>O Molecule for the (2 × 2)-N<sub>2</sub>O/Pd(110) Structures<sup>a</sup>**


structure	atom	$\Delta x$ (Å)	$\Delta y$ (Å)	$\Delta z$ (Å)
tilted on-top	Pd <sub>O</sub>	0.00	0.01	0.04
	Pd <sub>Nt</sub>	0.00	0.00	0.00
horizontal on-top	Pd <sub>O</sub>	0.00	-0.01	0.06
	Pd <sub>Nt</sub>	0.00	-0.02	0.02
tilted bridge	Pd <sub>O</sub>	-0.01	0.00	0.05
	Pd <sub>Nt</sub>	0.00	0.00	-0.01
horizontal bridge	Pd <sub>O</sub>	0.00	0.01	0.06
	Pd <sub>Nt</sub>	0.00	0.00	0.02

<sup>a</sup> The Cartesian coordinate system and the labels of surface Pd atoms are defined in the two plots above the table. The displacements ( $\Delta x$ ,  $\Delta y$ ,  $\Delta z$ ) are calculated with respect to the relaxed bare Pd(110) surface (i.e.,  $\Delta x = x_{\text{N}_2\text{O}/\text{Pd}(110)} - x_{\text{Pd}(110)}$ ).

top- and side-view snapshots of optimized structures are shown in Figure 3. Adsorption on the on-top site is energetically favorable for all probed N<sub>2</sub>O orientations with a typical on-top to bridge preference of 0.05–0.1 eV. Also the Pd–N distances are shorter for the on-top sites, being approximately 2.1 Å, with a little variation depending on super-cell geometry and coverage. The Pd–N distances of the bridge sites are typically 0.1 Å longer, being ~2.2 Å. A notable exception to this situation is the high coverage  $c(2 \times 2)$ , bridge-horizontally adsorbed N<sub>2</sub>O, because its Pd–N and Pd–O distances are substantially longer. This species is also 0.2 eV less stable than the on-top analogue, while at lower coverage it becomes stabilized and located much closer to the surface.

Although the Pd–O distances of horizontal N<sub>2</sub>O(a) species are about 0.2 Å longer than the Pd–N distances, the values of about 2.3 Å indicate that the horizontally adsorbed molecules also interact with the surface through the oxygen atom. This conclusion is supported by the accumulation of the charge in the Pd–O bonding region, as seen from the charge density difference,  $\Delta n(\mathbf{r}) = n_{\text{N}_2\text{O}/\text{sub}}(\mathbf{r}) - [n_{\text{sub}}(\mathbf{r}) + n_{\text{N}_2\text{O}}(\mathbf{r})]$ , displayed in Figure 4.

The adsorbate induces minor geometrical rearrangements (buckling) of the surface palladium atoms. In Table 3 the buckling parameters for (2 × 2)-N<sub>2</sub>O/Pd(110) structures are reported. The relaxations in the surface-normal direction are about 0.05 Å for the Pd<sub>Nt</sub> atoms and even smaller for the Pd<sub>O</sub> atoms (for the definition of the Pd<sub>Nt</sub> and Pd<sub>O</sub> labels see the inset in the Table 3). The lateral buckling is negligible since it is usually less than 0.01 Å.

## 4. Discussion

**4.1. Stable Adsorption.** Our GGA calculations indicate that N<sub>2</sub>O is adsorbed either with the terminal N atom attached to the surface or horizontally on the surface and in the [001] (or [00 $\bar{1}$ ]) direction. Notably, N<sub>2</sub>O adsorption at high (0.5 ML) and low (0.25ML) coverages displays similar stability, indicating the saturation coverage of N<sub>2</sub>O(a) to be at least 0.5 ML. This is in accord with experimental findings.<sup>5,15</sup> Adsorption on the on-top sites (0.36–0.40 eV) is energetically favorable and the bridge sites are less stable (0.18–0.29 eV). The stability of the on-top tilted and on-top horizontal forms are very similar at higher coverage, while at lower coverage the latter form is

slightly preferred. In contrast, the tilted form is more stable for the bridge sites (more particularly so at higher coverage). The molecule of the tilted adsorbed forms remains linear, whereas the horizontal N<sub>2</sub>O(a) becomes bent with its O atom pointing toward the surface.

The GGA is known to perform quite satisfactorily in many studies of strong chemisorption on metal surfaces (see, for example, refs 33 and 34). However, in the case of weak chemisorption, which is in part caused by dispersion interactions, the situation is not as good because the results are dependent on the choice of the GGA functional (see, for example, refs 35 and 36, and the references therein). Nevertheless, our GGA calculated binding energies are in good agreement with the experimentally estimated adsorption heat of 0.39 eV, which was obtained from the TDS (thermal desorption spectroscopy) peak temperature of N<sub>2</sub>O desorption (150 K),<sup>3</sup> assuming the simple first-order desorption and nonactivated adsorption<sup>37</sup> of N<sub>2</sub>O on Pd(110). Note that the PBE energy functional is known to give usually somewhat too large chemisorption energies.<sup>33</sup> Also the GGA is not able to describe the dispersion (i.e. van der Waals) interactions that are known to be the driving force for physisorption. In recent study of ammonia on the Au(111) surface,<sup>38</sup> the Perdew–Wang (PW91) functional<sup>39</sup> (which gives similar results as PBE) was found to yield a good geometry and binding energies, although the adsorbate–substrate interaction was found to be predominantly dispersive in nature. The PW91 and PBE functionals were suggested to be able to reproduce properties of some van der Waals systems,<sup>40,41</sup> but they do so empirically using covalent terms to mimic van der Waals ones<sup>38</sup> and are not generally reliable.<sup>35</sup>

It has frequently been proposed that the N–N bond in N<sub>2</sub>O(a) is inclined against the surface plane, on the basis of vibrational spectroscopy work on Pt(111) and Ir(111),<sup>42,43</sup> NEXAFS (near edge X-ray absorption fine structure spectroscopy) analysis of Ni(111)<sup>44</sup> and Cu(100),<sup>45</sup> and also use of the KIE (kinetic isotope effects) approach to polycrystalline Cu.<sup>46</sup> However, the angle of inclination is still unclear from experimental work, because there are difficulties in NEXAFS analysis which would provide the most reliable orientation. This admolecule shows two  $\pi$  resonance states and one broad  $\sigma$  resonance above the X-ray absorption edge of the nitrogen 1s state. The latter resonance was mostly suppressed when the molecule was on the surface. The former is due to the transition from the 1s state of the terminal and central nitrogen atoms to the 3 $\pi$  unoccupied state. This resonance intensity must change sharply with X-ray incidence angle when the N–N bond is oriented solely along one definite direction. However, the observed resonance intensity was commonly reported to be insensitive to X-ray incidence angle on the surfaces Ni(111), Cu(100), Ag(110) and Pd(110).<sup>44,45,47,48</sup> Two possible explanations cannot at present be differentiated with certainty. The first assumes only one adsorption form, proposed as a bent admolecule in which the N–N bond must largely incline from the surface normal.<sup>44,45</sup> In the second model, two adsorption forms, for example, a standing and lying one, are assumed. The lack of dependence on the incident angle is expected when the molecule can convert between the two forms.<sup>48</sup> The DFT results in this work are consistent with the second model.

We also investigated the electronic properties of the N<sub>2</sub>O chemisorption. The redistribution of the charge on adsorption, as well as the formation of a chemical bond between the adsorbate and substrate can be seen from Figure 4, where the charge density difference,  $\Delta n(\mathbf{r}) = n_{\text{N}_2\text{O}/\text{sub}}(\mathbf{r}) - [n_{\text{N}_2\text{O}}(\mathbf{r}) + n_{\text{sub}}(\mathbf{r})]$ , is plotted. Here,  $n_{\text{N}_2\text{O}/\text{sub}}(\mathbf{r})$ ,  $n_{\text{sub}}(\mathbf{r})$ , and  $n_{\text{N}_2\text{O}}(\mathbf{r})$  are the

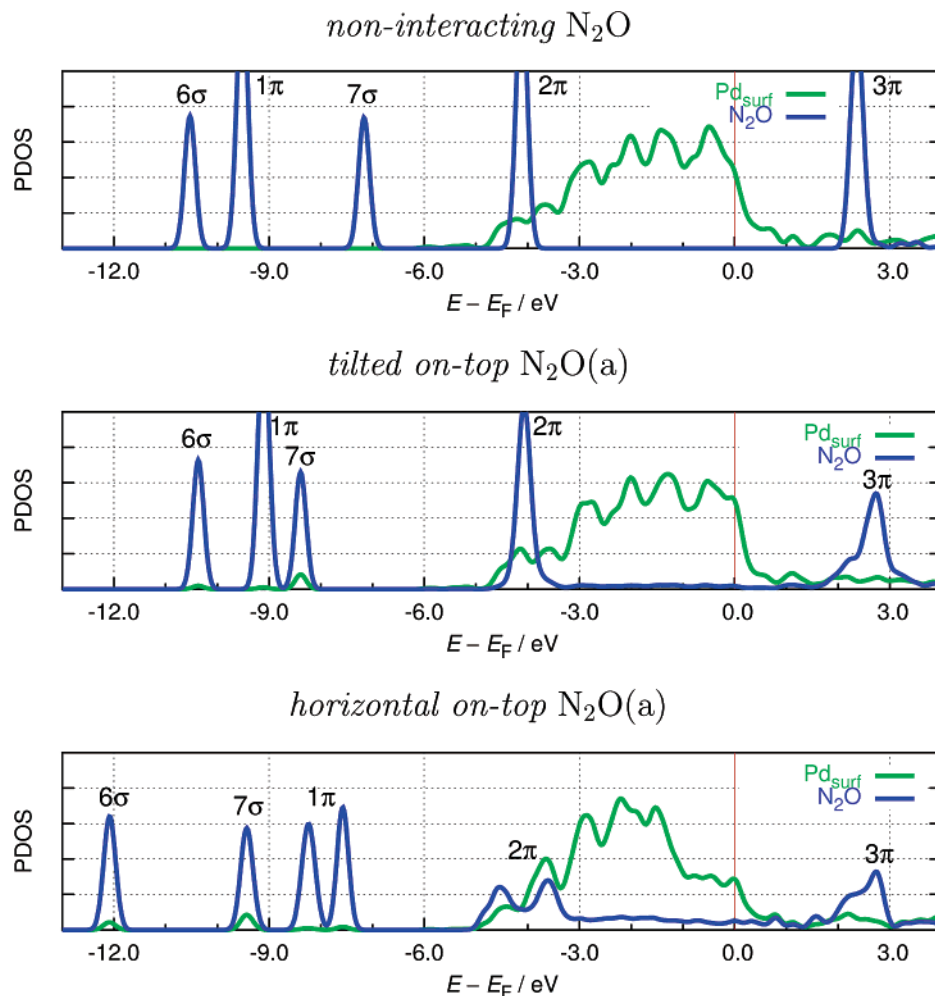


**Figure 5.** Density of states projected (PDOS) to the  $\text{N}_2\text{O}$  molecule and to the surface Pd atoms that interact with the  $\text{N}_2\text{O}$  molecule. The top part shows the PDOS for the “noninteracting” system (i.e., the  $\text{N}_2\text{O}$  is located  $\sim 6$  Å above the surface), the middle part shows the PDOS of the tilted on-top structure, while the bottom panel shows the PDOS for the horizontal on-top  $c(2 \times 2)\text{-N}_2\text{O}/\text{Pd}(110)$  structure. The characters of the derived molecular peaks of  $\text{N}_2\text{O}$  are also shown (labeling of the molecular states refer to the gas-phase  $\text{N}_2\text{O}$ ). Fermi level is chosen as the zero energy level for these plots.

electron charge density distributions of the  $\text{N}_2\text{O}$ -on-substrate, clean substrate, and  $\text{N}_2\text{O}$ , respectively. These plots show that the redistribution of the charge on adsorption is larger for the horizontal form. Moreover, they also show that the horizontal  $\text{N}_2\text{O(a)}$  species interact with the surface not only with the terminal nitrogen atom but also with the oxygen atom.

In Figure 5 we present the plots of the density of states projected (PDOS) to the  $\text{N}_2\text{O}$  molecule and to the surface Pd atoms that interact with the  $\text{N}_2\text{O}$  molecule for the tilted on-top and horizontal on-top  $c(2 \times 2)\text{-N}_2\text{O}/\text{Pd}(110)$  structures. An analogous PDOS plot is also shown for the “noninteracting” system (i.e., the  $\text{N}_2\text{O}$  is located  $\sim 6$  Å above the surface). By comparison of the two PDOS plots of interacting structures with that of the noninteracting one, we see that the PDOS of the tilted structure is affected only slightly by adsorption, while that of the horizontal structure is affected significantly more: a trend already found by the charge density difference plots (Figure 4). For the tilted on-top structure, the  $7\sigma$  molecular orbital is shifted down in energy, while the  $1\pi$  orbital is slightly upshifted. On the other hand, for the horizontal on-top structure  $6\sigma$  and  $7\sigma$  orbitals are downshifted, while  $1\pi$  orbitals are upshifted and split (also the  $2\pi$  orbitals are split). The  $7\sigma$  downshift and  $1\pi$  upshift are large enough, and the change in the relative order of these two states occurs. The PDOS plots indicate a weak coupling of (i) the molecular  $7\sigma$  orbital with unoccupied

substrate  $d_\sigma$  states (see note 49) and (ii) molecular  $2\pi$  orbitals with the  $d_\pi$  orbitals (see note 50) of the substrate. The substrate back-donation into the molecular antibonding  $3\pi$  is small for the horizontal form and absent for the tilted one. A similar bonding picture was proposed by Avery for the  $\text{N}_2\text{O}$  adsorption on  $\text{Pt}(111)$  surface.<sup>42</sup> A more detailed analysis of the electronic factors governing the adsorption process will be presented elsewhere.<sup>51</sup>

**4.2. Inclined Desorption.** On the basis of the experimentally observed inclined desorption of product  $\text{N}_2$  in the thermal decomposition of  $\text{N}_2\text{O(a)}$  on  $\text{Pd}(110)$  surface, two mechanisms were proposed,<sup>11</sup> one in which  $\text{N}_2\text{O(a)}$  was lying along the  $[001]$  direction, and the other in which  $\text{N}_2\text{O}$  was adsorbed by its O atom in a tilted form on a 3-fold hollow site in a trough. Our GGA calculations favor the horizontal form as the precursor for  $\text{N}_2\text{O}$  dissociation. This form of  $\text{N}_2\text{O(a)}$  is bent with its O atom pointing to the surface.

The horizontal form of  $\text{N}_2\text{O(a)}$  adsorbed on either the on-top or bridge site and lying in the  $[001]$  direction is acceptable as the precursor of dissociation, because the oxygen atom is easily released to the surface. The on-top horizontal  $\text{N}_2\text{O(a)}$  is more stable, although this does not exclude the bridge analogue. If we assume the dissociation to proceed via elongation of the N–O bond in the  $[001]$  direction—the direction of  $\text{N}_2$  desorption—then after the N–O bond is broken, the nascent O(a) is left



either near the on-top site (for the on-top N<sub>2</sub>O(a)) or near the bridge site (for the bridge N<sub>2</sub>O(a)). In the first case the O(a) is later on stabilized in the hcp-hollow site, while the second one is subsequently stabilized in the fcc-hollow site. Since the O(a) in the bridge (and fcc-hollow) site is more stable than in the on-top (and hcp-hollow) site, this contribution would favor the bridge path. Our preliminary calculations indicate that the total energies of the transition states might be similar for the two channels at 0.5 ML coverage. In this case dissociation would proceed mainly via the preferred channel, but also to a lesser extent, by the other. In particular, at 0.5 ML adsorbate coverage (i.e., for c(2 × 2) super-cell), the dissociation barrier for the paths across the on-top and bridge sites are 0.65 and 0.53 eV, respectively. Because experimental data indicate<sup>8,52</sup> that the activation energy of N<sub>2</sub>O(a) decomposition strongly depends on the coverage, the calculations of the N<sub>2</sub>O(a) dissociation at lower coverages are necessary, and are therefore underway.

## Conclusions

We have characterized in detail the adsorption structures predicted by DFT within the GGA approximation. The main results are that two stable forms are found, N<sub>2</sub>O being adsorbed either (i) in a tilted form with the terminal N atom attached to the surface or (2) lying horizontally on the surface. The two forms display very similar stabilities and prefer to adsorb on the on-top site and orient in the [001] direction. The binding energies of N<sub>2</sub>O(a) at higher (0.5 ML) and lower (0.25ML) coverages are similar.

The geometry of the tilted N<sub>2</sub>O molecule remains linear, and the molecular interatomic distances are almost unchanged on adsorption, while the geometry of the horizontal N<sub>2</sub>O is bent, with the O atom pointing toward the surface. Also the interatomic distances are longer than in the tilted form. The molecule-surface chemical interaction can be described by a weak coupling of (i) molecular 7σ orbital with the substrate d<sub>σ</sub> orbitals and (ii) molecular 2π orbitals with the d<sub>π</sub> orbitals of the substrate. The back-donation from the substrate into the antibonding 3π molecular orbitals was found to be larger for the horizontal form, although still very small, whereas back-donation for the tilted moiety is practically zero.

**Acknowledgment.** This work was supported financially by the Ministry of Education, Science and Sport of Slovenia, Grant No. P0-0544-0106, and in part by Grant-in-Aid No. 13640493 for General Scientific Research from the Japan Society for the Promotion of Science.

## References and Notes

- Kokalj, A.; Kobal, I.; Horino, H.; Ohno, Y.; Matsushima, T. *Surf. Sci.* **2002**, *506*, 196.
- Ohno, Y.; Kimura, K.; Bi, M.; Matsushima, T. *J. Chem. Phys.* **1999**, *110*, 8221.
- Ohno, Y.; Kobal, I.; Horino, H.; Rzeźnicka, I.; Matsushima, T. *Appl. Surf. Sci.* **2001**, *169–170*, 273.
- Ohno, Y.; Kobal, I.; Kimura, K.; Horino, H.; Matsushima, T. *Catal. Catal.* **1999**, *41*, 421.
- Horino, H.; Liu, S.; Ohno, Y.; Hiratsuka, A.; Matsushima, T. *Chem. Phys. Lett.* **2001**, *341*, 419.
- Matsushima, T. *Catal. Surv. Jpn.* **2002**, *5*, 71.
- Horino, H.; Liu, S.; Sano, M.; Wako, S.; Hiratsuka, A.; Ohno, Y.; Kobal, I.; Matsushima, T. *Top. Catal.* **2002**, *18*, 21.
- Horino, H.; Rzeźnicka, I.; Kobal, I.; Kokalj, A.; Matsushima, T.; Hiratsuka, A.; Ohno, Y. *J. Vac. Sci. Technol.* **2002**, *20*, 1592.
- Ikai, M.; He, H.; Borroni-Bird, C.; Hirano, H.; Tanaka, K. *Surf. Sci.* **1994**, *315*, L973.
- Ikai, M.; Tanaka, K. *Surf. Sci.* **1996**, *375*, 781.
- Kobal, I.; Kimura, K.; Ohno, Y.; Matsushima, T. *Surf. Sci.* **2000**, *445*, 472.
- Kobal, I.; Kimura, K.; Ohno, Y.; Horino, H.; Rzeźnicka, I.; Matsushima, T. *Stud. Surf. Sci. Catal.* **2000**, *130*, 1337.
- Rzeźnicka, I.; Ohno, Y.; Kobal, I.; Horino, H.; Kimura, K.; Matsushima, T. In *Proceedings of the 9th International Symposium Heterogeneous Catalysis*; Varna, Bulgaria, Sept 23–27, 2000; Petrov, L.; Bonev, C.; Kadinov, G., Eds.; Institute of Catalysis Bulgarian Academy of Sciences: Sofia, 2000.
- Ikai, M.; Tanaka, K. *J. Phys. Chem. B* **1999**, *103*, 8277.
- Haq, S.; Hodgson, A. *Surf. Sci.* **2000**, *463*, 1.
- Sano, M.; Ohno, Y.; Yamanaka, T.; Matsushima, T.; Quinay, B.; Jacobi, K. *J. Chem. Phys.* **1998**, *108*, 10231.
- Lee, J.; Kato, H.; Sawabe, K.; Matsumoto, Y. *Chem. Phys. Lett.* **1995**, *240*, 417.
- Perdew, J. P.; Burke, K.; Ernzerhof, M. *Phys. Rev. Lett.* **1996**, *77*, 3865.
- Vanderbilt, D. *Phys. Rev. B* **1990**, *41*, 7892.
- Monkhorst, H. J.; Pack, J. D. *Phys. Rev. B* **1976**, *13*, 5188.
- Methfessel, M.; Paxton, A. T. *Phys. Rev. B* **1989**, *40*, 3616.
- Baroni, S.; Dal Corso, A.; de Gironcoli, S.; Giannozzi, P. PWSCF and PHONON: Plane-Wave Pseudo-Potential Codes. <http://www.pwscf.org/>, 2001.
- Kokalj, A. *J. Mol. Graphics Modell.* **1999**, *17*, 176.
- Kokalj, A.; Causà, M. Scientific Visualization in Computational Quantum Chemistry. In *Proceedings of High Performance Graphics Systems and Applications European Workshop*; CINECA-Interuniversity Consortium: Bologna, Italy, 2000.
- Kokalj, A.; Causà, M. XCrySDen: (X-Window) CRYstalline Structures and DENsities. <http://www-k3.ijs.si/kokalj/xc/XCrySDen.html>, 2001.
- Kokalj, A. A Theoretical Study of Chemisorption and Reactions on Transition Metal Surfaces. Ph.D. Thesis, University of Ljubljana, 2000.
- Lide, D. R., Ed. *CRC Handbook of Chemistry and Physics*, 74th ed.; CRC Press: Boca Raton, FL, 1993.
- Kokalj, A.; Causà, M.; Dovesi, R. Unpublished data.
- Dong, W.; Ledentu, V.; Saute, P.; Kresse, G.; Hafner, J. *Surf. Sci.* **1997**, *377–379*, 56.
- Wandelt, K.; Gumhalter, B. *Surf. Sci.* **1984**, *140*, 355.
- Barnes, C. J.; Ding, M. Q.; Lindroos, M.; Diehl, R. D.; King, D. A. *Surf. Sci.* **1985**, *162*, 59.
- Lesar, A.; Hodošek, M. *J. Chem. Phys.* **1998**, *109*, 9410.
- Hammer, B.; Hansen, L. B.; Nørskov, J. K. *Phys. Rev. B* **1999**, *59*, 7413.
- Scheffler, M.; Stampfl, C. Theory of Adsorption on Metal Substrates. In *Handbook of Surface Science*; Horn, K.; Scheffler, M., Eds.; Elsevier: Amsterdam, 2000; Vol. 2.
- Vargas, M. C.; Giannozzi, P.; Selloni, A.; Scoles, G. *J. Phys. Chem. B* **2001**, *105*, 9509.
- Wu, X.; Vargas, M. C.; Nayak, S.; Lotrich, V.; Scoles, G. *J. Chem. Phys.* **2001**, *115*, 8748.
- Redhead, P. A. *Vacuum* **1962**, *12*, 203.
- Bilić, A.; Reimers, J. R.; Hush, N. S.; Hafner, J. *J. Chem. Phys.* **2002**, *116*, 8981.
- Perdew, J. P.; Wang, Y. *Phys. Rev. B* **1992**, *45*, 13244.
- Zhang, Y.; Pan, W.; Yang, W. *J. Chem. Phys.* **1997**, *107*, 7921.
- Adamo, C.; Barone, V. *J. Chem. Phys.* **1999**, *110*, 6158.
- Avery, N. R. *Surf. Sci.* **1983**, *131*, 501.
- Cornish, J. C. L.; Avery, N. R. *Surf. Sci.* **1990**, *235*, 209.
- Väterlein, P.; Krause, T.; Basler, M.; Fink, R.; Umbach, E.; Taborski, J.; Wüstenhagen, V.; Wurth, W. *Phys. Rev. Lett.* **1996**, *76*, 4749.
- Ceballos, G.; Wende, H.; Baberschke, K.; Arvantis, D. *Surf. Sci.* **2001**, *482–485*, 15.
- Polić, S.; Senegačnik, M.; Kobal, I.; Zieliński, M. *Pol. J. Chem.* **2001**, *75*, 1729.
- Horino, H.; Wako, S.; Matsushima, T.; Nagaoka, S.; Nakamura, E.; Tanaka, S.; Kamada, M. *UVSOR Activity Report*; Institute of Molecular Sciences: Okazaki, Japan, 2000; p 197.
- Horino, H. Unpublished data.
- The symbol d<sub>σ</sub> stands for the linear combination of atomic d<sub>z<sup>2</sup></sub> and s orbitals. In particular, the d<sub>σ</sub> orbitals of the surface Pd atoms located below the ad molecules are considered here.
- The symbol d<sub>π</sub> stands for either individual d<sub>xz</sub> or d<sub>yz</sub> atomic orbitals or the linear combination of the two. The d<sub>π</sub> orbitals have compatible symmetry with the π orbitals of the adsorbed molecule.
- Kokalj, A.; Kobal, I.; Matsushima, T. In preparation.
- Kobal, I.; Kokalj, A.; Horino, H.; Ohno, Y.; Matsushima, T. *Trends Chem. Phys.* **2003**, In press.